Optimal Combined Heat-and-Power Plant for a Low-Temperature Geothermal Source

Sarah Van Erdeweghe[a,c], Johan Van Bael[b,c], Ben Laenen[b], William D'haeseleer[a,c,*]

[a] *University of Leuven (KU Leuven), Applied Mechanics and Energy Conversion Section, Celestijnenlaan 300 - box 2421, B-3001 Leuven, Belgium*

[b] *Flemish Institute for Technological Research (VITO), Boeretang 200, B-2400 Mol, Belgium*

[c] *EnergyVille, Thor Park, Poort Genk 8310, B-3600 Genk, Belgium*

Abstract

This work compares the performance of four combined heat-and-power (CHP) configurations for application in a binary geothermal plant connected to a low-temperature 65/40 and a high-temperature 90/60 district heating system. The investigated configurations are the series, the parallel, the preheat-parallel and the HB4 configurations. The geothermal source conditions have been defined based on existing geothermal plants in the northwest of Europe. Production temperatures in the range of 110-150°C and mass flow rates in the range of 100-200kg/s are considered. The goal is to identify the best-performing CHP configuration for every set of geothermal source conditions (temperature and flow rate) and for multiple values of the heat demand. The electrical power output is used as the optimization objective and the different CHP plants are compared based on the exergetic plant efficiency. The optimal CHP plant has always a higher exergetic plant efficiency than the pure electrical power plant; up to 22.8%-pts higher for the connection to a 65/40 DH system and up to 20.9%-pts higher for the connection to a 90/60 DH system. The highest increase of the exergetic plant efficiency over the pure electrical power plant is obtained for low values of the geothermal source temperature and flow rate.

Keywords: CHP, district heating, geothermal, ORC, thermodynamic optimization

*Corresponding author
  Email address: william.dhaeseleer@kuleuven.be (William D'haeseleer)

1. Introduction

Deep-geothermal energy is a sustainable energy source which is continuously available, and independent of the weather conditions [1]. This is in strong contrast to, for example, wind and PV solar. However, in regions with a rather low geothermal source temperature (below $150°C$), the high drilling costs make these geothermal power plants not/hardly economically competitive without some kind of feed-in tariff. One way of improving the overall plant economics is by providing multiple types of energy outputs, rather than electrical power only. The exergetic plant efficiency [1] is frequently used for comparing the thermodynamic performance of multi-energy systems. Among others, low-temperature geothermal multi-energy systems have been recently studied in [2, 3, 4, 5, 6, 7, 8, 9, 10, 11, 12, 13, 14, 15, 16, 17, 18], the main points of which are now outlined:

Zare [2], Bellos et al. [3] and Islam et al. [4] have analyzed trigeneration systems, which provide heating, cooling and electricity. Zare [2] has conducted an thermodynamic optimization of two trigeneration systems, consisting of an Organic Rankine Cycle (ORC) or Kalina cycle, a LiBr/water absorption chiller and a heater for domestic hot water. The trigeneration cycles have been optimized towards maximal exergetic efficiency and reach values of 46.51% and 50.36% [1] for the ORC and the Kalina cycle implementation, respectively. Bellos et al. [3] have studied a trigeneration system based on a modified absorption heat pump. Part of the steam in the generator is extracted to flow through a steam turbine, thereby generating electrical power. The system is able to deliver heat, cold and electrical power, and has an exergetic efficiency of up to 72% [1]. Islam et al. [4] have proposed a hybrid solar-geothermal system consisting of two ORC power turbines, two thermal energy storage systems, a LiBr/water absorption chiller, a heat pump for space heating and a drying system. The authors have found overall energetic and exergetic efficiencies of 51% and 62%, respectively. Comparing with the exergetic efficiencies of a trigeneration, a cogeneration and a

---

[1]Different definitions for the exergetic efficiency η_{ex} can be found in the literature. In general, η_{ex} is defined as the ratio of the exergy content of the useful products and the exergy content of the energy sources. Mainly with respect to the exergy content of the geothermal energy source, differences exist. We prefer to use the flow exergy content of the geothermal energy source at the production well, rather than using the difference of the flow exergy content between the production and the injection wells. However, some references use the latter definition. They are indicated with the footnote number 1.

single generation system, η_{ex} is 1.6%-pts, 2%-pts and 8%-pts higher.

Calise et al. [5] and Mohammadi et al. [6] have added potable water production to the previous trigeneration system. The hybrid solar-geothermal system of Calise et al. [5] uses an ORC and is connected to a district heating and cooling network. The system provides electricity, desalinated water, heat and cooling energy for a cluster of 800 buildings on the Pantelleria island (Italy). Mohammadi et al. [6] have investigated a modified Kalina cycle coupled to a reverse osmosis system for the production of heating, cooling, electrical power and potable water with an exergetic efficiency of 38.1% [1]. Akrami et al. [7] and Boyaghchi et al. [8] have included the production of hydrogen to the trigeneration system. The system of Akrami et al. [7] consists of an ORC, a LiBr/water absorption cooling system, a domestic water heater and a proton exchange membrane. The overall energy and exergetic efficiencies are 34.98% and 49.17%. Boyaghchi et al. [8] have proposed a cascaded set-up of an ORC, a liquefied natural gas (LNG) vaporization process and a proton exchange membrane. An exergetic efficiency of 38.2% can be obtained.

Akbari Kordlar et al. [9], Mosaffa et al. [10], Oyewunmi et al. [11] and Fiaschi et al. [12] have presented a geothermally-fueled cogeneration system, for only two desired output products. Akbari Kordlar et al. [9] have proposed a combined cooling-and-power (CCP) system, consisting of an ORC and an absorption refrigerator. The authors have optimized the CCP system for thermodynamic and economic objectives. If the system is optimized towards maximal exergetic plant efficiency, $\eta_{ex} = 36.1\%$ can be obtained [1]. Mosaffa et al. [10] have performed a thermoeconomic analysis of four types of ORC systems with the vaporization of LNG as a heat sink. The operating conditions have been optimized towards maximal energetic efficiency, maximal exergetic efficiency [1] or minimal product cost. The authors have concluded that the ORC with internal heat recuperator is preferable with respect to the other set-ups (simple ORC, regenerative ORC, dual-fluid ORC). Depending on the optimization objective, exergetic plant efficiencies [1] of 36-40% are obtained. Oyewunmi et al. [11] have evaluated the performance of working fluid mixtures in an ORC system, where the condenser heat is used for heating purposes (e.g., district heating). They have investigated several source temperatures (low: $150°C$, medium: $250°C$ and high: $330°C$), representing multiple types of heat sources. The authors conclude that the use of mixtures is especially favorable for high supply temperatures ($90°C$) of the heat demand due to the temperature glide in the condenser. For the low-temperature energy source ($150°C$) — which we will also consider in this work —, they have

presented exergetic efficiencies [1] higher than 50% or 60% for heating supply temperatures of $45°C$ and $90°C$, respectively. Fiaschi et al. [12] have proposed a low- to medium-temperature (130-170$°C$) geothermal combined heat-and-power (CHP) system which delivers heat at higher temperatures for industrial use. The operating conditions of their so-called *Cross Parallel CHP* have been optimized towards maximal net electrical power output while satisfying the heat utility demand by means of genetic algorithms. With respect to the parallel configuration, the Cross Parallel CHP can reach an improvement of up to 55% in net electrical power output for the investigated conditions, with corresponding exergetic efficiency of 70-78% [1].

In this work, we focus on the utilization of a low-temperature geothermal energy source for the combined production of electricity and heat delivery to a nearby district heating system. Several types of CHP plants are possible. References [13, 14, 15, 16], e.g., have studied the performance of the parallel and/or series CHP plants, fueled by a low-temperature heat source. It was found that the series CHP plant is the most favorable for the connection to a low-temperature district heating (DH) system and high source temperatures, whereas the parallel configuration is more appropriate for the connection to high-temperature district heating systems and lower source temperatures. In general, the exergetic efficiency is higher for the CHP plants than for a pure electrical power plant, whereas the pure electrical power plant reaches a higher electrical power output. A different CHP type is the preheat-parallel configuration as proposed by Van Erdeweghe et al. in [17]. This type is a combination of the series and the parallel configurations. The preheat-parallel configuration can produce a higher electrical power output than the series and parallel configurations for a wide range of supply and return temperatures of the district heating system. For a brine [2] temperature of 130$°C$ and flow rate of 194kg/s, and for the connection to a 75/50 [3] DH system with a heat demand of 6MWth, the electrical power output of the preheat-parallel configuration is 3.11% and 5.25% higher than for the parallel and series configurations, respectively. A fourth CHP type is the HB4 configuration as proposed by Habka et al. in [18]. The authors have proposed four CHP configurations fueled by a geothermal brine at a temperature of 100$°C$ and a flow rate of 1kg/s. A 75/50 DH system has been considered with a heat demand of $110 - 170$kW. For the investigated boundary conditions, all CHP configurations have shown higher values of the exergetic

---

[2]Brine is another name for the geothermal fluid, since it is water with some dissolved gasses, minerals, ...

[3]$T_{supply} = 75°C$ and $T_{return} = 50°C$.

plant efficiency, while the stand-alone electrical power plant produces more electricity. The authors indicate that the HB4 configuration could become the state-of-the-art configuration for CHP plants fueled by geothermal water due to its simplicity and its ability to cool down the geothermal source to a low temperature.

In this paper, the main goal is to compare the performance of the most promising CHP configurations — the series, the parallel, the preheat-parallel and the HB4 configuration — for the application in a binary geothermal CHP plant connected to a third or fourth generation district heating system. The best-performing CHP configuration will be indicated based on the electrical power output and the exergetic plant efficiency, and depends on the brine and district heating system conditions. In this study, we consider geothermal brine temperatures in the range of 110-150$°C$ and flow rates in the range of 100-200kg/s. These values are based on existing binary geothermal projects in the northwest of Europe (especially in Germany [19]). Furthermore, based on the existing power plants [19] and on the recent IRENA report on *Renewable energy in district heating and cooling* [20], the temperatures of the DH systems are determined; a high-temperature (third generation) 90/60 DH system for existing districts — where houses are heated by conventional space heating systems — and a low-temperature (fourth generation) 65/40 DH system for new districts — where houses are connected via floor heating systems or heat pumps. The ORC technology is considered for the heat-to-electricity conversion.

The novelty of this paper lies in the wide range of investigated geothermal source conditions (based on the geology of the Balmatt geothermal site in Belgium [21]), the discussion for two common types of district heating systems and the comparison of the series, the parallel, the *preheat-parallel* and the *HB4* CHP layout. The convenient series and parallel layouts have been widely discussed in the literature and were also subject of previous work by the authors [16]. Based on the series and parallel CHP layouts, the authors have presented the so-called *preheat-parallel* CHP layout in [17] and have shown its potential for application in binary geothermal CHP plants. Finally, Habka et al. [18] have proposed the *HB4* CHP layout and concluded that this CHP layout may become the state-of-the-art for geothermal applications. Therefore, we want to investigate its potential for the source conditions in the northwest of Europe (110-150$°C$ and 100-200kg/s), which are different from the conditions of the study of Habka et al. [18] (100$°C$ and 1kg/s). The most appropriate CHP layout will be indicated, and depends on the brine and DH system conditions.

2. Methodology

2.1. Set-up of the CHP configurations

Figure 1 gives a schematic outline of the investigated CHP configurations: the series, the parallel, the preheat-parallel and the HB4 CHP. In the series CHP, the entire brine flow rate delivers heat to the ORC at the brine production temperature and subsequently to the DH system at a lower temperature. In the parallel configuration, part of the brine delivers heat to the ORC and part of the brine delivers heat to the DH system, both at the brine production temperature but at different flow rates. The preheat-parallel configuration is a combination of the series and the parallel CHP types. The brine delivers heat to the ORC at the production temperature and the remaining heat is delivered to the DH system to heat the DH water from the return temperature (T_{return}) to an intermediate temperature (T_{mid}). To reach the supply temperature (T_{supply}), part of the brine is used to deliver heat in the parallel branch. The HB4 configuration resembles the series CHP, but the difference is that the brine flow rate is split after having delivered heat to the evaporator of the ORC. Afterwards, part of the brine is used in the ORC preheater and part of the brine is used to satisfy the heat demand of the DH system. The temperature at which the brine delivers heat to the DH system is higher compared to the series CHP and lower compared to the parallel CHP.

2.2. Optimization model

The objective of the optimization model is to maximize the electrical power output of the ORC $\dot{W}$, while satisfying the heat demand of the district heating system $\dot{Q}_{DH}$. The electrical power output of the ORC is defined as:

$$\dot{W} = \dot{W}_t \eta_g - \dot{W}_p / \eta_m, \tag{1}$$

with $\dot{W}_t$ and $\dot{W}_p$ the turbine and pump mechanical power, and η_g and η_m the generator and motor efficiencies. The mechanical power of the turbine and pump are calculated as:

$$\dot{W}_t = \dot{m}_{wf} \left(h_3 - h_4 \right) \quad \text{and} \quad \dot{W}_p = \dot{m}_{wf} \left(h_2 - h_1 \right), \tag{2}$$

with $\dot{m}_{wf}$ the working fluid mass flow rate, and h the specific enthalpy. The subscripts indicate the working fluid states and follow the nomenclature of Figure 1. The heat transfer in the DH system

6
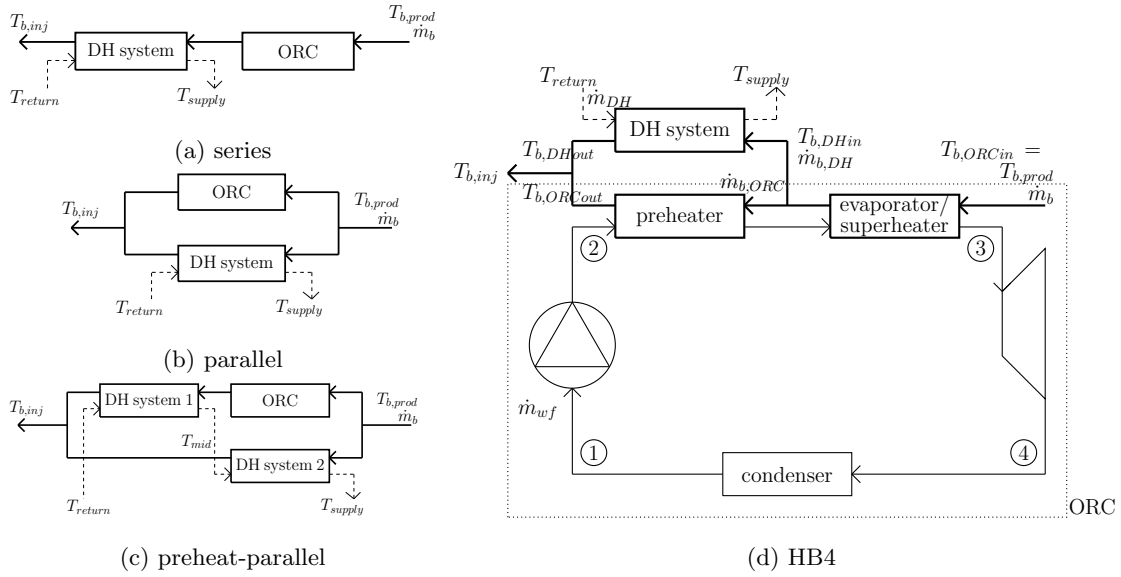
Figure 1: Schematic outline of the series, the parallel, the preheat-parallel [17] and the HB4 [18] CHP configurations. The dashed lines indicate the district heating water. The ORC schematic outline is presented together with the HB4 configuration. However only a basic ORC is shown in the figure, also ORCs with internal heat recovery (recuperated) are considered.

heat exchanger is modeled as follows:

$$\dot{m}_{DH}\left(h_{supply} - h_{return}\right) = \dot{m}_{b,DH}\left(h_{b,DHin} - h_{b,DHout}\right), \tag{3}$$

with $\dot{m}_{DH}$ the flow rate of the DH system water and $\dot{m}_{b,DH}$ the brine flow rate in the branch of the DH system; the subscripts DH in and DH out indicate the brine inlet and outlet state of the DH system heat exchanger, respectively. The heat transfer in all other heat exchangers is modeled in a similar way. Mixing occurs in the parallel, the preheat-parallel and the HB4 CHP plants. As an example, the mixing in the HB4 CHP is modeled as (following the nomenclature of Figure 1):

$$\dot{m}_b = \dot{m}_{b,ORC} + \dot{m}_{b,DH} \tag{4}$$

$$\dot{m}_b h_{b,inj} = \dot{m}_{b,ORC} h_{b,ORCout} + \dot{m}_{b,DH} h_{b,DHout} \tag{5}$$

The different CHP plants will be compared based on the exergetic plant efficiency, which is defined as:

$$\eta_{ex} = \frac{\dot{W} + \dot{E}_{DH}}{\dot{E}_{b,prod}}, \tag{6}$$

in which $\dot{E}_{DH}$ and $\dot{E}_{b,prod}$ are the flow exergy of the heat delivered to the district heating system and the flow exergy content of the brine at the production state, respectively. The flow exergy $\dot{E}$ is generally defined as:

$$\dot{E} = \dot{m}\left[h - h_0 - T_0\left(s - s_0\right)\right], \tag{7}$$

with s the specific entropy, T the temperature and subscript 0 indicating the dead state. The dead state values cancel out for $\dot{E}_{DH}$ since only differences apply.

2.3. Assumptions

The model results are based on the following assumptions [16, 17, 22]:

- a subcritical ORC with a minimal degree of superheating of $0.01°C$ to be able to calculate the ORC fluid properties;

- a minimal temperature difference of $\Delta T_{pinch} = 5°C$;

- no pressure drops in the heat exchangers;

8

- isentropic turbine and pump efficiencies of $\eta_t = 85\%$ and $\eta_p = 80\%$;

- generator and motor efficiencies of $\eta_g = 98\%$ and $\eta_m = 98\%$;

- a condenser temperature of $T_{cond} = 25°C$;

- the cooling water inlet state: $T_{c,in} = 12°C$ and $p_{c,in} = 2bar$;

- the dead state: $T_0 = 15°C$ and $p_0 = 1bar$;

Furthermore, the brine has been modeled as pure water.

2.4. Implementation and validation

The models are implemented in Python [23] and the optimal operating conditions — temperatures and mass flow rates — are found using the CasADi [24] optimization framework, coupled to the IpOpt non-linear solver [25]. The fluid properties have been called from the REFPROP [26] database. The net electrical power output $\dot{W}$ is the optimization objective.

The exergetic plant efficiency η_{ex} is used as a performance indicator. η_{ex} is defined in Eq. (6) as the ratio of the useful outputs (net electrical power $\dot{W}$ and heat — taking into account the temperature levels, so the exergy content of heat asked by the district heating system, $\dot{Ex}_{DH}$) to the available flow exergy content of the brine in the production state ($\dot{Ex}_{b,prod}$). This definition is different from some definitions in the modern literature, as discussed in footnote [1]. However, we opt for using the exergy content of the brine at the production state ($\dot{Ex}_{b,prod}$) as a reference instead of the difference in flow exergy between the production and the injection states ($\dot{Ex}_{b,prod} - \dot{Ex}_{b,inj}$). The flow exergy content of the brine at the production state is the available exergy which can be used and, in our definition, the exergy content of the injected brine exergy is considered as a loss.

The validation results of the ORC and the series and parallel CHP models were given in [16]. No experimental data have been found for the preheat-parallel configuration, however the validated ORC model has been used. The HB4 configuration model results were validated in [27] against the results of Habka et al. [18].

	MW [g/mole]	T_{crit} [$°C$]	p_{crit} [bar]	ODP	GWP	atm. life [years]
R236ea	152.04	139.3	35.0	0	1410	11

Table 1: Thermodynamic and environmental properties of the ORC working fluid R236ea [29].

2.5. ORC fluid

R236ea is chosen as the ORC working fluid since it results in a high electrical power output of a pure electrical power plant at reference brine conditions [16, 28]. Table 1 shows its thermodynamic and environmental properties [29].

3. Results

First, the reference conditions for the geothermal source conditions, the heat demand and some cycle parameters are given. Then, a parameter study is performed to show the impact of the type of district heating system, the cycle parameters, the brine conditions and the heat demand on the plant performance. Finally, scaling issues are taken into account. Scaling is the phenomenon of salt sedimentation on the well pipes or heat exchanger surfaces and has to be avoided in order to maintain a proper operation of the power/CHP plant. Due to scaling issues, a constraint on the brine temperature might be imposed. Furthermore, a proper reservoir exploitation and safety measures might impose additional constraints on the brine (injection) temperature (both, upper and lower bounds).

3.1. Reference values

The reference values for the brine temperature and flow rate, the heat demand and the most important cycle parameters (condenser temperature, pinch-point-temperature difference and isentropic turbine efficiency) are given in Table 2. The minimum and maximum values correspond to the range of variation in the parameter study (Section 3.2).

10

parameter	min. value	reference value	max. value
brine temperature, $T_{b,prod}$ [$°C$]	110	130	150
brine mass flow rate, $\dot{m}_b$ [kg/s]	100	150	200
heat demand, $\dot{Q}_{DH}$ [MWth]	5	10	20
condenser temperature, T_{cond} [$°C$]	20	25	30
pinch-point-temperature difference, ΔT_{pinch} [$°C$]	2	5	10
isentropic turbine efficiency, η_t [%]	80	85	90

Table 2: Reference values of the brine temperature and flow rate, the heat demand and the most important cycle parameters. The minimum and maximum values correspond to the range of variation in the parameter study (Section 3.2).

3.2. Parameter study

In this parameter study, the effect of the type of district heating system on the CHP performance as well as the effect of the important cycle parameters, the brine conditions and the heat demand are subsequently investigated.

3.2.1. Type of district heating system

Figure 2 gives the electrical power output of the four investigated CHP systems (that were shown in Figure 1) as a function of the heat demand. Two types of DH systems are considered; the connection to a 65/40 DH system on the left-hand side (LHS) and the connection to a 90/60 DH system on the right-hand side (RHS). *P, S, PP* and *HB4* are the abbreviations for the parallel, the series, the preheat-parallel and the HB4 configuration. The horizontal black line presents the power output of a pure electrical power plant for the same (reference) brine conditions. The ORC implementation can be of the basic type (as presented in Figure 1) or of the recuperated type (internal heat recuperation between the working fluid at state 4 and state 2 via an extra heat exchanger). The recuperated cycle has a higher cycle efficiency due to the internal heat recovery. Since for the series and preheat-parallel configurations the heat addition to the ORC depends on the temperature levels of the DH system, the recuperated cycle has been used (indicated by *recup* in the legend of Figure 2). The ORC performance in the parallel configuration does not depend on the DH system temperatures, so that the basic and the recuperated ORC lead to the same electrical

(a) 65/40 DH system   (b) 90/60 DH system
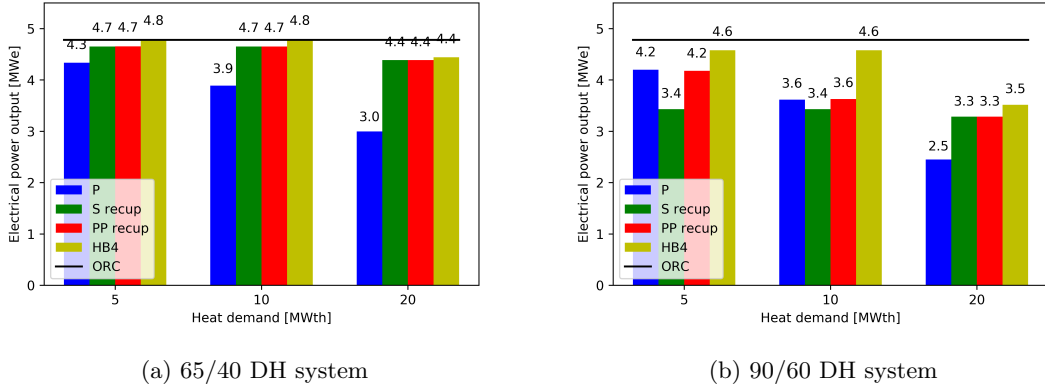
Figure 2: Electrical power output of the four CHP configurations for the brine and ORC system reference conditions (of Table 2), but for the three listed values of the heat demand, 5, 10 and 20MWth. The pure electrical power plant (black horizontal line) is given for comparison. For a color version of this figure, the reader is referred to the online version of this paper.

power output. The basic cycle has been considered because of its simplicity. The electrical power output of the HB4 configuration with basic and recuperated ORC is the same, so that also here the basic cycle has been considered.

For the low-temperature 65/40 DH system, Figure 2 LHS shows that the series CHP performs better than the parallel CHP, which is consistent with the results found in the literature. Furthermore, the preheat-parallel configuration reduces to the series set-up. The HB4 configuration has the highest electrical power output, and is even capable of producing as much electricity as a pure electrical power plant for a heat demand of 5 and 10MWth. For the high heat demand of 20MWth, all CHP configurations produce less electricity than a pure electrical power plant.

For the connection to a 90/60 DH system (Figure 2, RHS), the parallel CHP performs better than the series CHP due to the high temperatures of the DH system. However, for high values of the heat demand, the series CHP might have a higher electrical power output. This can be explained as follows. For a high heat demand, a high brine flow rate is needed in the parallel branch (high $\dot{m}_{b,DH}$ — see Figure 1) and the brine flow rate going to the ORC branch ($\dot{m}_{b,ORC}$) is low. As a result, also the ORC electrical power output is low. On the other hand, in case of the series CHP, the entire brine flow rate provides heat to the ORC. The brine ORC outlet temperature $T_{b,ORCout}$

12

is constrained due to the supply temperature of the DH system. For a high heat demand, the effect of the mass flow rate is more important than the constraint on the ORC outlet temperature so that the series CHP has a higher electrical power output than the parallel CHP. As for the 65/40 DH system, the HB4 configuration is able to produce more electricity while satisfying the heat demand.

So, in conclusion, for both types of DH systems and for the reference brine conditions, the HB4 configuration has the highest electrical power output and the highest exergetic plant efficiency.

3.2.2. Cycle parameters

Figure 3 shows the influence of the condenser temperature, the pinch-point-temperature difference and the isentropic turbine efficiency on the electrical power output of the power/CHP plants. The reference values for the brine conditions, the heat demand and the non-varying cycle parameters are considered (see Table 2), so that only one variable has been changed at a time.

Consider the low-temperature 65/40 DH system first (Figure 3, LHS). It is clear from the figures that the HB4 configuration has the highest electrical power output, which equals the power output of the pure electrical power plant. Therefore the corresponding (yellow and black) lines collapse. The series CHP (and the preheat-parallel CHP which reduces to the series configuration — so the green and the red lines collapse) has the second highest electrical power output. The parallel configuration is performing the worst. When no dashed line are visible, that means that they are identical to the solid lines.

Second, for the 90/60 DH system, shown on the RHS of Figure 3, the HB4 configuration is still the best-performing CHP but does not reach the electrical power output of a pure electrical power plant anymore due to the higher temperatures of the heat demand. The HB4 configuration is now followed by the parallel configuration and the series configuration, respectively. The preheat-parallel configuration reduces to the parallel CHP.

In general, a lower condenser temperature, a lower pinch-point-temperature difference and a higher isentropic turbine efficiency lead to a higher ORC cycle efficiency hence a higher electrical power output. Of course, a thermoeconomic analysis has to be performed in order to determine the optimal values for T_{cond}, ΔT_{pinch} and η_t. A lower condenser temperature goes together with a

13

(a) 65/40 DH system   (b) 90/60 DH system
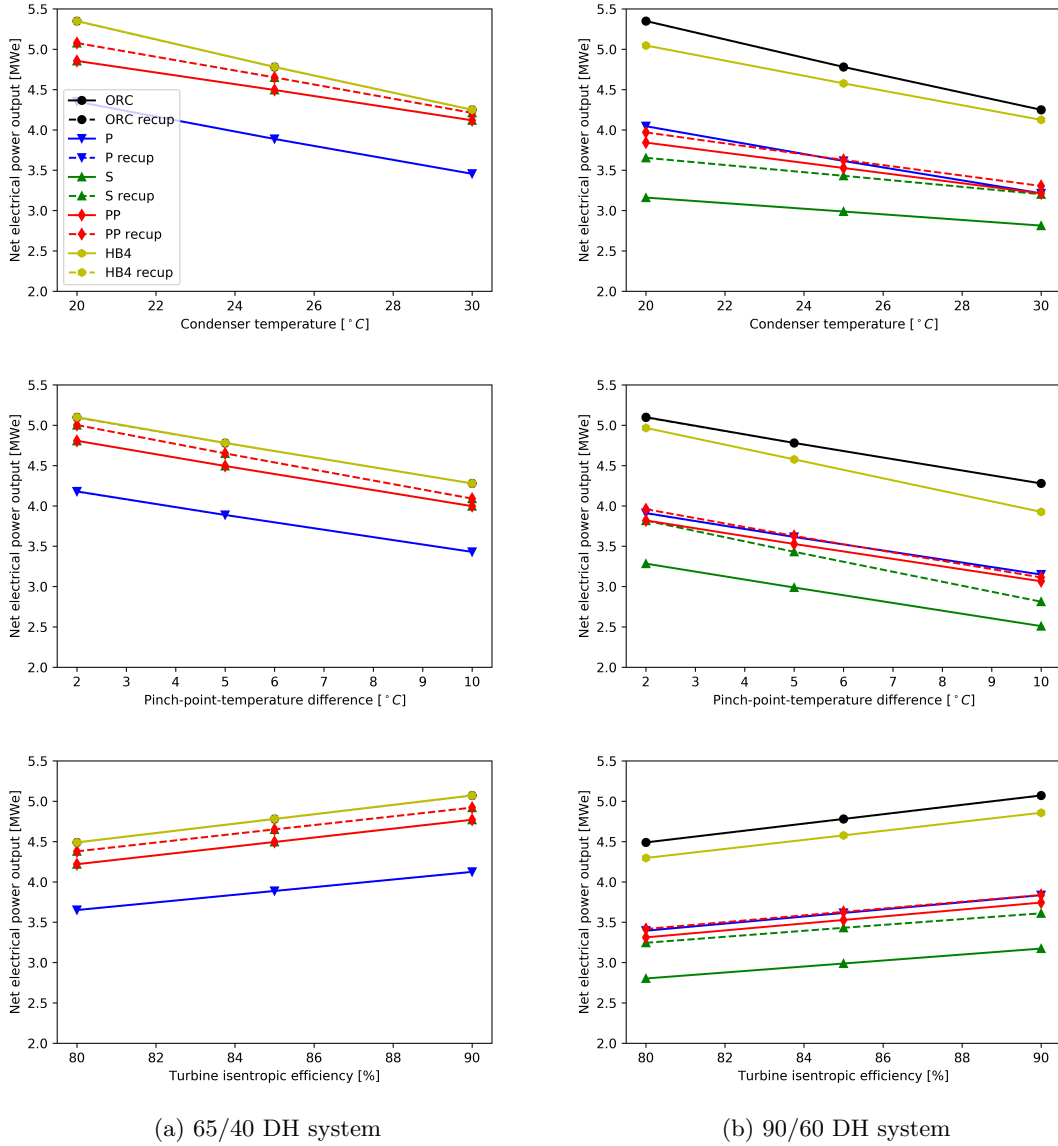
Figure 3: Electrical power output of the four CHP configurations and the pure electrical power plant as a function of the condenser temperature, the pinch-point-temperature difference and the turbine isentropic efficiency, for reference brine conditions and a heat demand of $\dot{Q}_{DH} = 10MWth$, for the two DH systems: 65/40 (LHS) and 90/60 (RHS). For a color version of this figure, the reader is referred to the online version of this paper.

larger and more expensive cooling installation, a lower pinch-point-temperature difference would give rise to bigger and more expensive heat exchangers and a more efficient turbine is more costly. In this study, we give an indication on how the cycle performance would change by varying these parameters; however, a full thermoeconomic analysis is required to find the *optimal* values which belong to the most economic plant. Thermoeconomic model implementation and optimization of the CHP plants are planned for future work.

3.2.3. Brine conditions

Here, we discuss the effect of the brine conditions on the pure electrical power plant and on the performance of the CHP plants.

Pure electrical power plant

Figure 4 shows the electrical power output (full lines) and the exergetic plant efficiency (dashed lines) of the pure electrical power plant as a function of the brine temperature and flow rate. The electrical power output increases with the source temperature and increases linearly with the brine flow rate. The exergetic plant efficiency is independent of the brine flow rate so that all dashed lines in the figure coincide. This can be seen from the definition of η_{ex} in Eq. (6). The electrical power output $\dot{W}$ increases linearly with $\dot{m}_b$ and also the brine flow exergy at the production state $\dot{E}_{b,prod}$ increases linearly with $\dot{m}_b$. Since the heat demand is zero in case of a pure electrical power plant, the linear dependencies on the brine flow rate in the numerator and the denominator of Eq. (6) cancel out. Furthermore, both the power output and the brine exergy content increase with the production temperature. But the increase in electrical power output dominates such that the exergetic plant efficiency increases with $T_{b,prod}$.

CHP plants for the reference heat demand of 10MWth

The pure electrical power plant performance is taken as the point of comparison for the different CHP configurations. Since heat delivery comes into play, the exergetic plant efficiency of the CHP plants will depend on the mass flow rate (for a given constant heat demand). The exergy of the heat demand is added in the numerator of Eq. (6) such that the brine flow rates in the definitions of $\dot{W}$ and $\dot{E}_{b,prod}$ do not cancel out anymore.

15
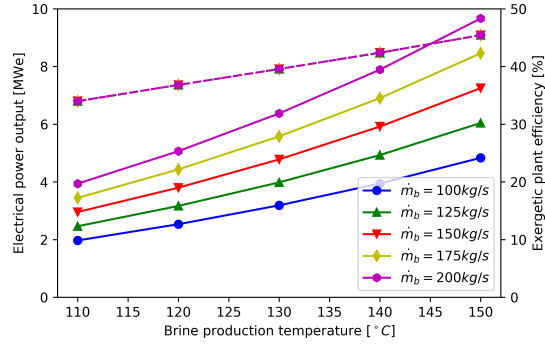
Figure 4: Electrical power output (full lines and LHS ordinate scale) and exergetic plant efficiency (dashed lines and RHS ordinate scale) of the pure electrical power plant as a function of the brine production temperature and brine flow rate. For a color version of this figure, the reader is referred to the online version of this paper.

270 The performance of each individual CHP configuration type is discussed as a function of the brine production temperature and flow rate and for the reference heat demand of $\dot{Q}_{DH} = 10MWth$. The loss in electrical power output and the gain in exergetic plant efficiency compared to a pure electrical power plant (with shown characteristics in Figure 4) are presented in Figures 5 and 6 [4], for the connection to a 65/40 and a 90/60 DH system, respectively.

275 From Figure 5 it follows that the electrical power output is always lower than or equal to that of a pure electrical power plant, while the exergetic plant efficiency is higher for all cases considered. Especially at low values of the brine mass flow rate and at low brine temperatures, the gain in exergetic plant efficiency due to the heat delivery is outspoken. In general, the loss in electrical power output diminishes as the brine production temperature is higher. At higher values of $T_{b,prod}$, 280 the share of the brine energy (and exergy) content which is used for heat delivery is lower, hence the electrical power production is less influenced by the heat delivery.

For the parallel configuration, the loss in electrical power output depends on the brine mass flow rate. Since the entire brine flow rate $\dot{m}_b$ has to be divided over the ORC branch and the heat

_____

[4]The figures on the left-hand side show the *loss in electrical power output with respect to a pure ORC*, so the higher the value the lower the electrical power output of the CHP plant (so a low value is better). On the right-hand side, we show *the gain in exergetic plant efficiency with respect to a pure ORC*, so the higher the value, the better and the higher the exergetic plant efficiency.
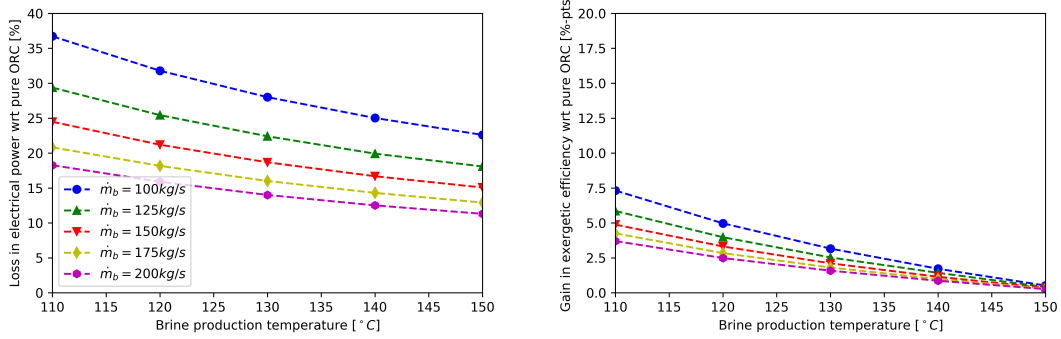
(a) Parallel CHP
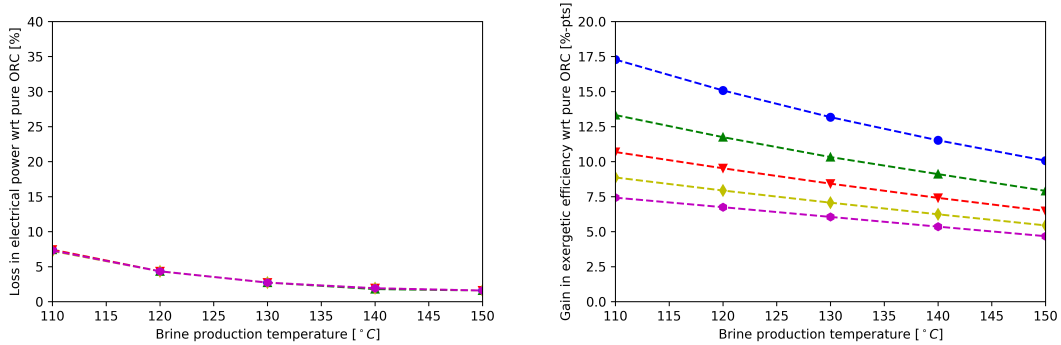
(b) Recuperated series CHP
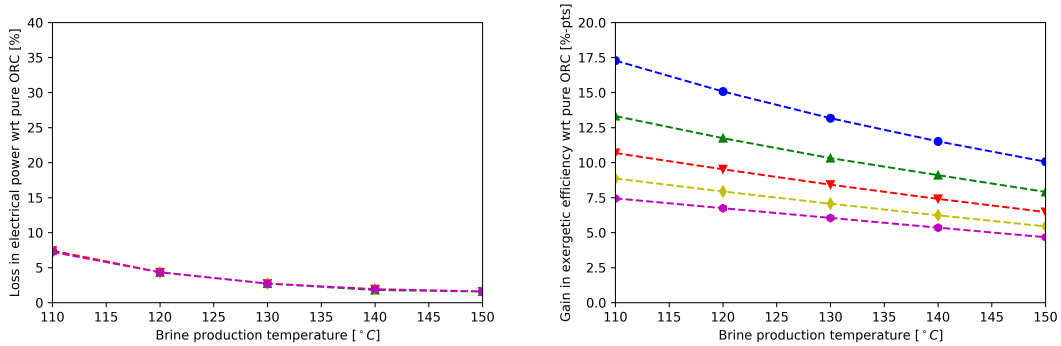
(c) Recuperated preheat-parallel CHP
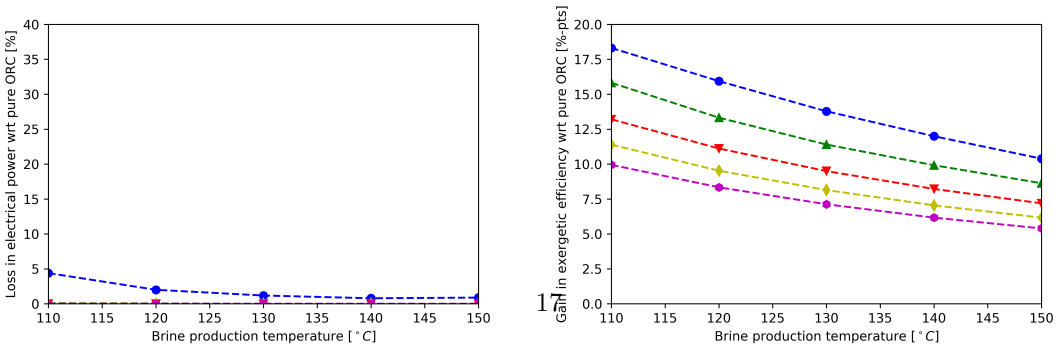
(d) HB4 CHP

Figure 5: Loss in electrical power output and gain in exergetic plant efficiency compared to the pure electrical power plant as a function of the brine production temperature and flow rate, for the connection to a **65/40 DH system** and the reference heat demand of $\dot{Q}_{DH} = 10MWth$. For a color version of this figure, the reader is referred to the online version of this paper.

delivery branch, the loss in electrical power output is higher for lower brine flow rates. The loss in electrical power output of the series CHP with respect to the pure electrical power plant is independent of the brine mass flow rate (as long as the heat demand is not too high or the brine flow rate too low). The preheat-parallel configuration reduces to the series CHP and the results are the same. The HB4 configuration is capable of generating as much electricity as the pure electrical power plant for almost all investigated brine conditions. Only at the low brine flow rate of 100kg/s, the electrical power production is slightly lower (up to 5% lower for $T_{b,prod} = 110°$C) than for the pure electrical power plant.

Figure 6 shows the analogue results but for the connection to a high-temperature 90/60 DH system. We see that the loss in electrical power output is still the highest at low values of the brine flow rate and low brine production temperatures. Also, less electrical power output is produced for the connection to a high-temperature DH system (compare the values in Figure 6 with these of Figure 5). The HB4 configuration is capable of providing as much electricity as a pure electrical power plant for high brine mass flow rates (175kg/s and 200kg/s) and high brine production temperatures ($140°C$ and $150°C$).

As before, the parallel configuration power output difference depends on both $T_{b,prod}$ and $\dot{m}_b$, whereas the series CHP electrical power output difference does not depend on the flow rate. However, for the series configuration, the trends for the gain in exergetic plant efficiency (RHS figures) have changed. There exists an optimal value for $T_{b,prod}$ which results in maximal exergetic plant efficiency. This can be explained as follows. For low values of the production temperature, the electricity generation is very low. By increasing the production temperature, more electricity can be generated. The exergy content of the brine increases as well, but slower so the overall exergetic plant efficiency increases. For higher values of $T_{b,prod}$, the exergy content of the brine still increases but the electrical power output does not increase that fast (the trend LHS figure flattens). And the overall exergetic plant efficiency decreases. So there exists an optimum for $T_{b,prod}$ which corresponds to the maximal exergetic plant efficiency.

For the connection to the 90/60 DH system, the preheat-parallel configuration does no longer reduce to the series configuration. This is illustrated by Figure 7, which shows the share of the total heat demand which is delivered in DH HEx 1 (nomenclature of Figure 1), the heat exchanger in the ORC branch. The series and the parallel CHP are two limiting cases of the preheat-parallel
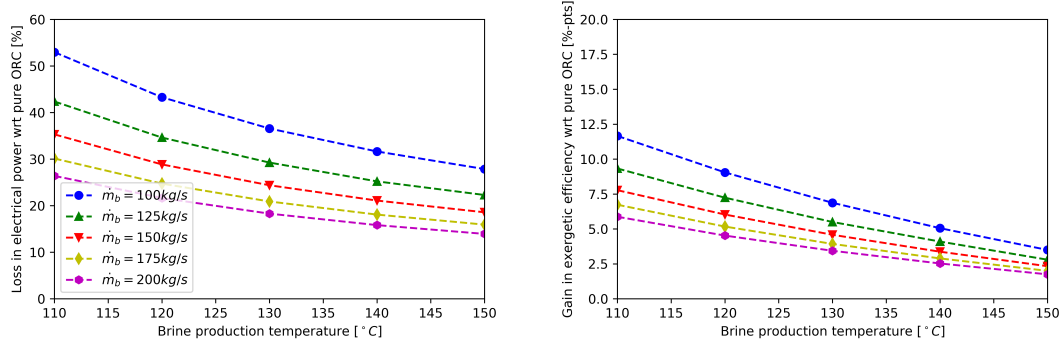
18

(a) Parallel CHP

(b) Recuperated series CHP

(c) Recuperated preheat-parallel CHP

19
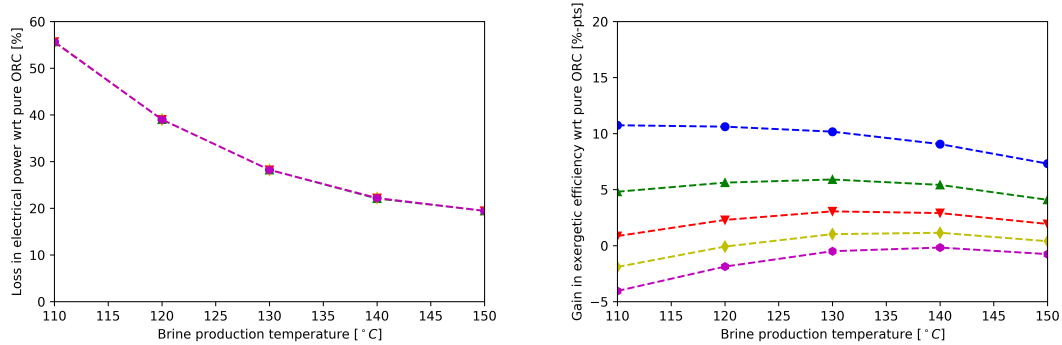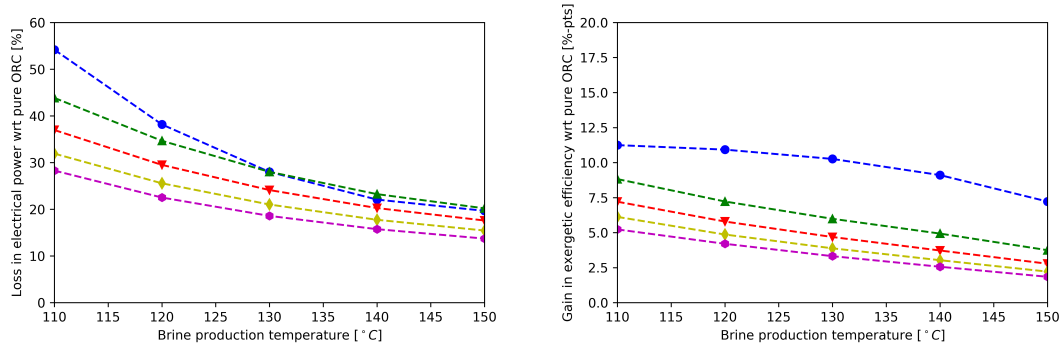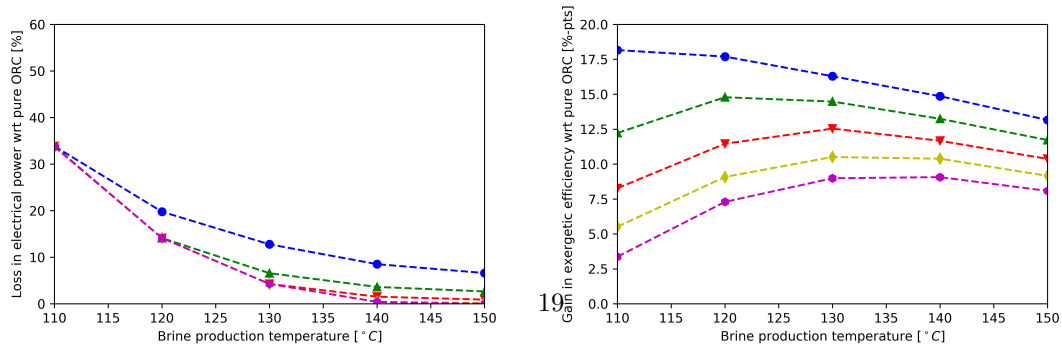
(d) HB4 CHP

Figure 6: Loss in electrical power output and gain in exergetic plant efficiency compared to the pure electrical power plant as a function of the brine production temperature and flow rate, for the connection to a **90/60 DH system** and the reference heat demand of $\dot{Q}_{DH} = 10MWth$. For a color version of this figure, the reader is referred to the online version of this paper.
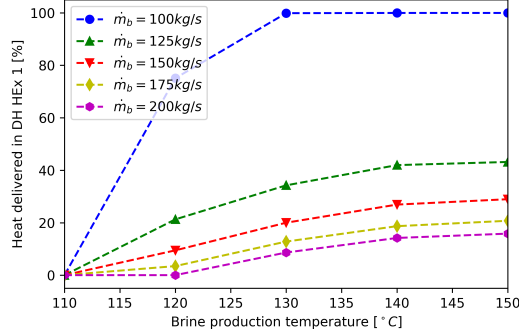
Figure 7: Share of the heat delivered in the ORC branch heat exchanger — DH HEx 1 — of the preheat-parallel configuration, as a function of the brine conditions and for the reference heat demand of $\dot{Q}_{DH} = 10MWth$. For a color version of this figure, the reader is referred to the online version of this paper.

configuration with $\dot{Q}_{DH1}/\dot{Q}_{DH} = 1$ and $\dot{Q}_{DH1}/\dot{Q}_{DH} = 0$, respectively. From Figure 7, we see that the preheat-parallel CHP reduces to the series CHP for low brine flow rates and high brine production temperatures, whereas it reduces to the parallel configuration at low values of the brine production temperature. For intermediate values, part of the total heat demand is delivered in DH HEx 1 in the ORC branch and part of it in DH HEx 2 in the parallel branch. The according plant performance was already given in Figure 6.

The trends for the HB4 configuration are similar to the trends for the series CHP layout, but the impact on the plant performance is lower. This is because the temperature of heat delivery to the DH system is already higher than for the series CHP.

From the RHS panels of Figure 6 it is clear that the exergetic plant efficiency of the parallel, the preheat-parallel and the HB4 CHP's is higher than that of a pure electrical power plant with the same brine conditions. However, the series CHP might have lower exergetic plant efficiency than a pure electrical power plant, especially for high brine flow rates. So it is clear that the series CHP is not suitable for the connection to a DH system operating at high temperatures. The HB4 is again the best-performing CHP since it has the lowest loss in electrical power output compared to a pure electrical power plant and the highest exergetic plant efficiency.

20

3.2.4. Influence of the heat demand

Table 3 shows the exergetic plant efficiency of the best-performing CHP plant as a function of the brine temperature, brine flow rate and heat demand, for the connection to a 65/40 DH system. The bottom line gives the exergetic efficiency of a pure electrical power plant. From Table 3 it follows that the HB4 configuration (slots without shading) is the optimal CHP configuration for almost all the investigated brine conditions and heat demands. Only at high heat demands and low brine flow rates, the series configuration (green shade in Table 3) might have a better performance. In this case, it is important to use the entire brine flow rate for driving the ORC.

$\dot{Q}_{DH}$ ↘	$T_{b,prod} = 110°C$			$T_{b,prod} = 120°C$			$T_{b,prod} = 130°C$			$T_{b,prod} = 140°C$			$T_{b,prod} = 150°C$		
$\dot{m}_b$	5	10	20	5	10	20	5	10	20	5	10	20	5	10	20
100kg/s	43.9	52.3	56.8	45.2	52.8	57.6	46.7	53.4	58.3	48.6	54.4	58.7	50.8	55.8	59.0
125kg/s	41.9	49.8	56.8	43.5	50.1	57.0	45.3	51.0	56.9	47.3	52.3	57.3	49.8	54.1	58.1
150kg/s	40.6	47.2	55.3	42.4	47.9	55.1	44.3	49.1	55.8	46.5	50.6	56.5	49.0	52.6	57.4
175kg/s	39.7	45.3	53.6	41.6	46.3	54.1	43.7	47.7	54.5	45.9	49.5	55.3	48.5	51.6	56.6
200kg/s	39.0	43.9	52.1	41.0	45.2	52.6	43.1	46.7	53.4	45.5	48.6	54.3	48.1	50.8	55.8
	$\eta_{ex,ORC} = 34.0\%$			$\eta_{ex,ORC} = 36.8\%$			$\eta_{ex,ORC} = 39.6\%$			$\eta_{ex,ORC} = 42.4\%$			$\eta_{ex,ORC} = 45.4\%$		

Table 3: The exergetic plant efficiency of the optimal CHP as a function of the brine production temperature, the brine mass flow rate and the heat demand $\dot{Q}_{DH}$ (in MWth), for the connection to a **65/40 DH system**. Slots without shading: HB4 CHP is optimal, green shading: series CHP is optimal. For a color version of this table, the reader is referred to the online version of this paper.

Furthermore, we see that the exergetic plant efficiency increases with the brine production temperature, decreases with the brine flow rate rate and strongly increases with the heat demand. The highest increase of the exergetic plant efficiency with respect to a pure electrical power plant is observed for the series CHP at ($T_{b,prod} = 110°C$, $\dot{m}_b = 100kg/s$ and $\dot{Q}_{DH} = 20MWth$) and is 22.8%-pts.

The equivalent results for the connection to a 90/60 DH system are shown in Table 4: the exergetic plant efficiency of the best-performing CHP plant as a function of the brine temperature, brine flow rate and heat demand. As for the 65/40 DH system, the exergetic plant efficiency increases with a higher brine temperature, with a lower brine flow rate and with a higher heat demand.

The HB4 configuration (slots without shading) is again optimal for almost all the investigated conditions. However at low brine temperatures and low heat demands, the parallel configuration (blue shading) might have a higher electrical power output, hence a higher η_{ex}. At low source temperatures and for the connection to this high-temperature DH system, the heat addition to the ORC in case of the HB4 configuration is limited. In case of the parallel configuration, the ORC electrical power output does not depend on the temperatures of the heat demand. Only a small fraction of the brine flow rate is required in the parallel branch to satisfy low demands such that the ORC electrical power output can be kept high.

$\dot{Q}_{DH}$ ↘	$T_{b,prod} = 110°C$			$T_{b,prod} = 120°C$			$T_{b,prod} = 130°C$			$T_{b,prod} = 140°C$			$T_{b,prod} = 150°C$		
$\dot{m}_b$	5	10	20	5	10	20	5	10	20	5	10	20	5	10	20
100kg/s	39.8	52.2	-	44.1	54.5	57.6	48.6	55.9	59.1	51.5	57.3	60.0	53.5	58.6	60.7
125kg/s	38.7	46.2	54.9	41.6	51.6	57.0	46.4	54.1	58.3	49.6	55.6	59.6	51.9	57.2	60.7
150kg/s	37.9	42.3	54.8	39.9	48.3	56.4	45.0	52.1	57.5	48.4	54.1	58.8	50.8	55.8	59.9
175kg/s	37.3	40.7	53.6	39.4	45.9	55.2	44.0	50.1	56.7	47.5	52.8	58.1	50.1	54.6	59.2
200kg/s	36.9	39.8	52.2	39.1	44.1	54.5	43.2	48.6	55.6	46.9	51.5	57.3	49.5	53.5	58.6
	$\eta_{ex,ORC} = 34.0\%$			$\eta_{ex,ORC} = 36.8\%$			$\eta_{ex,ORC} = 39.6\%$			$\eta_{ex,ORC} = 42.4\%$			$\eta_{ex,ORC} = 45.4\%$		

Table 4: The exergetic plant efficiency of the optimal CHP as a function of the brine production temperature, the brine mass flow rate and the heat demand $\dot{Q}_{DH}$ (in MWth), for the connection to a **90/60 DH system**. Slots without shading: HB4 CHP is optimal, blue shading: parallel CHP is optimal. For a color version of this table, the reader is referred to the online version of this paper.

The highest gain in exergetic plant efficiency over a pure electrical power plant is 20.9%-pts and is obtained for the HB4 configuration at ($T_{b,prod} = 110°C$, $\dot{m}_b = 125kg/s$ and $\dot{Q}_{DH} = 20MWth$). As a remark, the slot ($T_{b,prod} = 110°C$, $\dot{m}_b = 100kg/s$ and $\dot{Q}_{DH} = 20MWth$) is empty because the brine flow exergy at these conditions is too low to satisfy a heat demand of 20MWth at these high temperatures.

It is instructive to compare the values of η_{ex} for the optimal CHP connected to a 65/40 system (Table 3) with the values for the connection to a 90/60 DH system (Table 4). At low brine temperatures, the values of η_{ex} for the connection to a 65/40 DH system are higher than these for the 90/60 DH system. At lower temperatures of the DH system, the potential for electricity generation of the CHP plant

is higher, which results in a higher exergetic efficiency. However, at higher source temperatures, the difference between the electricity-generating potential for different temperatures of the DH system is less outspoken. The electricity produced will be (slightly) lower for the connection to a 90/60 DH system, however the higher exergy content of heat at higher temperatures is the dominating effect on η_{ex}. So for high values of the brine production temperature, the exergetic efficiency for the connection to a 90/60 DH system is generally higher than for the connection to a 65/40 DH system — mainly due to the higher exergy content of the heat source.

For the investigated conditions, the exergetic plant efficiency of the optimal CHP plant is always higher than for the corresponding pure electrical power plant. This indicates that the low-temperature geothermal source can be used more efficiently in a CHP plant configuration than in a pure electrical power plant and that the plant economics might be increased by providing useful heat.

3.3. Influence of a brine temperature constraint

Due to dissolved gasses or minerals in the geothermal water (brine), scaling might occur in the piping or heat exchangers. Since scaling lowers the heat transfer rate and thereby the efficiency and power output of the CHP plants, this has to be avoided. Therefore, and depending on the brine composition, the brine temperature might be constrained to a value which is higher than the optimal brine injection temperature. Furthermore, a proper reservoir exploitation and safety measures might impose additional constraints on the brine temperature (both, upper and lower bounds). In this section, we want to investigate the impact of a constraint on the brine temperature on the performance of the power plant and CHP configurations. In general, the brine injection temperature is determined by the brine composition. For the brine conditions at the Balmatt geothermal site in Mol (Belgium), the optimal injection temperature is higher than the constraint imposed by the brine composition, so no constraint has to be considered. However, at other location, that constraint might have to be taken into account. The constraint $T_b \geq 70°C$ has been chosen because it is mentioned in several studies, e.g., [30, 31, 32, 33].

23

3.3.1. Reference conditions

Figure 8 presents the performance of the four investigated CHP plants and the pure electrical power plant for the reference brine and system conditions and for three values of the heat demand. The connection to a low-temperature 65/40 DH system is shown on the left-hand side, the connection to a high-temperature 90/60 DH system on the right-hand side. This is a similar setup as Figure 2. As in Figure 2, the black line indicates the power output of a pure electrical power plant. In this case the pure electrical power plant with a recuperated ORC is considered as a reference. The constraint on the brine temperature makes that the brine can not be cooled down until the optimal injection temperature, which is lower than $70°C$ for the considered working fluid. The heat addition to the ORC is therefore constrained and the highest ORC efficiency and the highest electrical power output are obtained with the recuperated ORC. For the same reason, all CHP configurations have the highest electrical power output for the implementation with a recuperated ORC.

The electrical power output of the (recuperated) pure electrical power plant is $\dot{W} = 4.49MWe$ instead of $\dot{W} = 4.78MWe$ in case of no constraint on the brine temperature. Furthermore, from Figure 8 it follows that the series and HB4 configurations perform almost equally well for the connection to a 65/40 DH system whereas the parallel CHP has a lower electrical power output. Due to the constraint on the brine temperature, the HB4 CHP is no longer capable of generating the same electrical power output as a pure electrical power plant. For the connection to a 90/60 DH system, the HB4 configuration has the highest electrical power output for the heat demands of 5MWth and 10MWth. In this case, the same electrical power output is reached as for the connection to a low-temperature 65/40 DH system. For the high heat demand of 20MWth, the HB4 and the series configurations perform equally well and the electrical power output is lower.

3.3.2. Pure electrical power plant

Figure 9 shows the electrical power output and the exergetic plant efficiency of the pure electrical power plant as a function of the brine production temperature and flow rate, and taking the brine temperature constraint into account: $T_b \geq 70°C$. As mentioned before, the recuperated ORC has a better performance than the basic cycle due to the internal heat recuperation and the according higher cycle efficiency. The full lines indicate the electrical power output of the recuperated ORC, the dashed lines indicate the corresponding exergetic plant efficiency and the dotted lines the

24

(a) 65/40 DH system   (b) 90/60 DH system
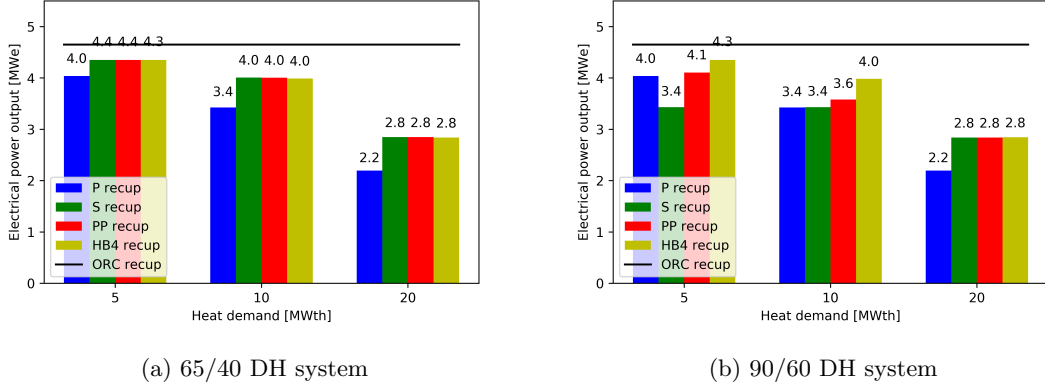
Figure 8: Electrical power output of the four CHP configurations for the brine and ORC system reference conditions (of Table 2), but for the three listed values of the heat demand, 5, 10 and 20MWth. The pure electrical power plant (black horizontal line) is given for comparison and the constraint on the brine temperature: $T_b \geq 70^\circ C$ is accounted for. For a color version of this figure, the reader is referred to the online version of this paper.

performance of the basic cycle. Compared to the basic cycle, the exergetic plant efficiency of the recuperated ORC is higher by 2.52%-pts and 0.72%-pts at $T_{b,prod} = 110^\circ$C and $T_{b,prod} = 150^\circ$C, respectively. So especially at low brine temperatures, the gain by using a recuperated ORC is the highest.

3.3.3. CHP plants

Table 5 shows the exergetic plant efficiency of the best-performing CHP as a function of the brine production temperature, the brine flow rate and the heat demand, for the connection to a low-temperature 65/40 DH system and taking into account the constraint on the brine temperature. The exergetic plant efficiency of the pure electrical power plant (with recuperated ORC) is given at the bottom line for comparison reasons. We can see that η_{ex} increases with $T_{b,prod}$. This is by analogy with the results without brine temperature constraint (Table 3). However, from Table 5 we can observe that η_{ex} decreases with the brine flow rate at low heat demands but η_{ex} increases with $\dot{m}_b$ at high heat demands. At low values of $\dot{m}_b$, η_{ex} shows an optimum as a function of the heat demand. At first, increasing the heat demand gives an extra utilization of the geothermal energy source without decreasing the electrical power output too much. However, at higher heat demands the electrical power output is decreased strongly such that η_{ex} decreases. For high values of the

25
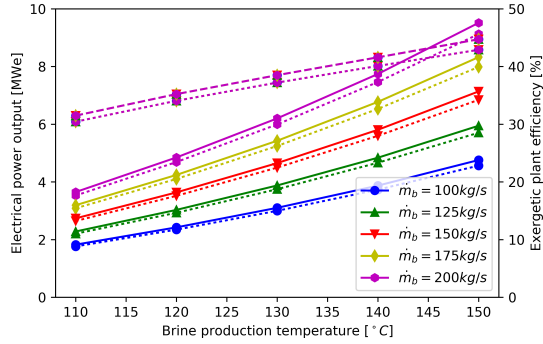
Figure 9: Electrical power output (full lines and LHS ordinate scale) and exergetic plant efficiency (dashed lines and RHS ordinate scale) of the pure (recuperated) electrical power plant as a function of the brine production temperature and the brine flow rate, including the brine temperature constraint: $T_b \geq 70°C$. The dotted lines indicate the performance of a basic ORC implementation. For a color version of this figure, the reader is referred to the online version of this paper.

435 brine flow rate, η_{ex} increases with the heat demand for all investigated brine conditions.

In contrast to Table 3, we can conclude from Table 5 that now the series configuration (green shading) is almost always the best-performing CHP configuration for the connection to a 65/40 DH system and the imposed constraint on the brine temperature. In some cases, the HB4 CHP shows a better performance. But, the differences in electrical power output and in exergetic plant efficiency
440 with respect to the series configuration are below 0.78% and 0.26%-pts, respectively.

Table 6 presents the exergetic plant efficiency of the best-performing CHP as a function of the brine production temperature, the brine flow rate and the heat demand, for the connection to a high-temperature 90/60 DH system and taking into account the constraint on the brine temperature. We can see that η_{ex} increases with $T_{b,prod}$ and decreases with $\dot{m}_b$. Furthermore η_{ex} increases with
445 the heat demand. Taking the brine temperature constraint into account, the values of η_{ex} for the connection to a high-temperature DH systsem are always higher than these for the connection to a low-temperature DH system. This is logical since the temperature levels of the heat demand are closer to the source temperature such that the energy source can be used more efficiently.

In general, the HB4 CHP has the highest electrical power output. There are two exceptions. The
450 preheat-parallel configuration (red shading) has the highest electrical power output for $T_{b,prod} =$

26

$\dot{\mathbf{Q}}_{\mathbf{DH}} \searrow$	$\mathbf{T_{b,prod}=110°C}$			$\mathbf{T_{b,prod}=120°C}$			$\mathbf{T_{b,prod}=130°C}$			$\mathbf{T_{b,prod}=140°C}$			$\mathbf{T_{b,prod}=150°C}$		
$\mathbf{\dot{m}_b}$	**5**	**10**	**20**	**5**	**10**	**20**	**5**	**10**	**20**	**5**	**10**	**20**	**5**	**10**	**20**
100kg/s	35.9	36.0	-	39.3	40.1	35.6	41.7	43.4	39.1	44.2	45.9	41.2	46.7	47.8	45.0
125kg/s	35.5	36.3	33.7	38.6	40.2	37.8	41.2	43.2	41.3	43.7	45.3	44.4	46.4	47.4	47.2
150kg/s	35.0	36.3	34.9	38.0	40.0	39.0	40.8	42.7	42.6	43.5	44.8	45.6	46.2	47.1	48.1
175kg/s	34.6	36.1	35.6	37.7	39.7	39.7	40.5	42.1	43.1	43.3	44.4	46.0	46.1	46.8	48.1
200kg/s	34.3	35.9	36.0	37.4	39.3	40.1	40.3	41.7	43.4	43.1	44.2	45.9	46.0	46.7	47.8
	$\eta_{\mathbf{ex,ORC}}=\mathbf{31.5}\%$			$\eta_{\mathbf{ex,ORC}}=\mathbf{35.2}\%$			$\eta_{\mathbf{ex,ORC}}=\mathbf{38.5}\%$			$\eta_{\mathbf{ex,ORC}}=\mathbf{41.6}\%$			$\eta_{\mathbf{ex,ORC}}=\mathbf{44.7}\%$		

Table 5: The exergetic plant efficiency of the optimal CHP as a function of the brine production temperature, the brine mass flow rate and the heat demand $\dot{Q}_{DH}$ (in MWth), for the connection to a **65/40 DH system** and a constraint on the brine temperature: $T_b \geq 70°C$. Slots without shading: HB4 CHP is optimal, green shading: series CHP is optimal. For a color version of this table, the reader is referred to the online version of this paper.

110°C and for a low heat demand. The electrical power output is only 1.35% (at $\dot{m}_b = 200kg/s$) to 4.30% (at $\dot{m}_b = 100kg/s$) higher than that of the parallel CHP, which is the second best configuration. For a heat demand of 20MWth, the series CHP (green shading) has the best performance for all $\dot{m}_b \leq 175kg/s$, although the HB4 configuration can reach almost the same electrical power output.

4. Conclusions

In this work, we have investigated the performance of four CHP configurations — the parallel, the series, the preheat-parallel and the HB4 configurations — fueled by geothermal energy with a temperature and flow rate of 110-150°C and 100-200kg/s. Two types of district heating systems have been considered: a 90/60 DH system where houses are heated by conventional heating systems and a 65/40 DH system where houses are heated by heat pumps or floor heating systems. We have found that the exergetic efficiency of the optimal CHP plant is always higher than the exergetic efficiency of a pure electrical power plant. This is especially the case for low temperatures and low flow rates of the geothermal energy source. For the investigated conditions, the exergetic plant efficiency can be increased by up to 22.8%-pts ($\eta_{ex} = 56.8\%$) and 20.9%-pts ($\eta_{ex} = 54.9\%$) compared to a pure electrical power plant for the connection to a low-temperature 65/40 and a

$\dot{Q}_{DH}$ ↘	$T_{b,prod} = 110°C$			$T_{b,prod} = 120°C$			$T_{b,prod} = 130°C$			$T_{b,prod} = 140°C$			$T_{b,prod} = 150°C$		
$\dot{m}_b$	5	10	20	5	10	20	5	10	20	5	10	20	5	10	20
100kg/s	37.9	45.7	-	42.9	48.3	52.2	45.5	50.4	53.3	47.2	52.0	54.5	49.3	53.1	55.7
125kg/s	36.6	44.1	49.4	41.3	46.8	51.1	44.0	48.9	52.7	46.2	50.1	54.3	48.5	51.7	55.8
150kg/s	35.6	42.0	48.0	39.9	45.4	50.1	43.1	47.2	52.0	45.5	48.9	53.8	48.0	50.6	55.2
175kg/s	35.0	39.3	46.8	38.2	44.0	49.2	42.5	46.1	51.2	45.0	47.9	52.9	47.6	49.9	54.1
200kg/s	34.6	37.9	45.7	37.7	42.9	48.3	42.0	45.3	50.4	44.6	47.2	52.0	47.3	49.3	53.1
	$\eta_{ex,ORC} = 31.5\%$			$\eta_{ex,ORC} = 35.2\%$			$\eta_{ex,ORC} = 38.5\%$			$\eta_{ex,ORC} = 41.6\%$			$\eta_{ex,ORC} = 44.7\%$		

Table 6: The exergetic plant efficiency of the optimal CHP as a function of the brine production temperature, the brine mass flow rate and the heat demand $\dot{Q}_{DH}$ (in MWth), for the connection to a **90/60 DH system** and a constraint on the brine temperature: $T_b \geq 70°C$. Slots without shading: HB4 CHP is optimal, green shading: series CHP is optimal, red shading: preheat-parallel CHP is optimal. For a color version of this table, the reader is referred to the online version of this paper.

high-temperature 90/60 DH system, respectively.

In general, the HB4 CHP configuration has the best performance. However, for a low-temperature DH system, the series CHP might have a higher electrical power output for low values of the brine flow rate and high heat demands. For a high-temperature DH system, the parallel CHP might have a better performance for a low value of the brine production temperature and low heat demands.

Taking into account a constraint on the brine temperature of $T_b \geq 70°C$, the series CHP is generally the most appropriate configuration for the connection to a 65/40 DH system. For the connection to a 90/60 DH system, the HB4 has the highest electrical power output for almost all investigated conditions. However, at high heat demands and for low to medium brine flow rates, the series CHP performs slightly better and for low values of $T_{b,prod}$ and low heat demands, the preheat-parallel CHP has a better performance.

For future work, we plan to implement thermoeconomic models for the proposed CHP systems. Based on these thermoeconomic optimization model results, we will be able to compare the economics of the different CHP configurations and identify the most economic CHP plant.

Acknowledgments

485 **Nomenclature**

Symbols and abbreviations

symbol	description
%-pts	percentage points
CHP	Combined Heat-and-Power
DH	District Heating
$\dot{E}$ [MWth]	flow exergy
GWP	Global Warming Potential
h [kJ/kg]	specific enthalpy
HB4	HB4 CHP set-up as defined in [18]
$\dot{m}$ [kg/s]	mass flow rate
MW [g/mole]	molecular weight
ODP	Ozone Depletion Potential
ORC	Organic Rankine Cycle
p [bar]	pressure
$\dot{Q}$ [MWth]	heat
s [kJ/kgK]	specific entropy
T [°C]	temperature
$\dot{W}$ [MWe]	electrical power
η [%]	efficiency

Subscripts & superscripts

symbol	description
0	dead state
1	wf state at pump inlet
2	wf state at pump outlet
3	wf state at turbine inlet
4	wf state at turbine outlet
b	brine
c	cooling water
$cond$	condenser
$crit$	critical point
DH	District Heating system
e	electrical
ex	exergetic
g	generator
in	inlet
inj	injection state
m	motor
ORC	Organic Rankine Cycle
out	outlet
p	pump
$pinch$	pinch point
$prod$	production state
$return$	return state DH system
$supply$	supply state DH system
t	turbine
th	thermal
wf	working fluid

References

[1] R. Bertani, Perspectives for Geothermal Energy in Europe, World Scientific (Europe), 2017. URL: `http://www.worldscientific.com/worldscibooks/10.1142/q0069`. doi:`10.1142/q0069`.

[2] V. Zare, A comparative thermodynamic analysis of two tri-generation systems utilizing low-grade geothermal energy, Energy Conversion and Management 118 (2016) 264–274.

[3] E. Bellos, C. Tzivanidis, K. A. Antonopoulos, Parametric investigation and optimization of an innovative trigeneration system, Energy Conversion and Management 127 (2016) 515–525.

[4] S. Islam, I. Dincer, Development, analysis and performance assessment of a combined solar and geothermal energy-based integrated system for multigeneration, Solar Energy 147 (2017) 328–343.

[5] F. Calise, A. Macaluso, A. Piacentino, L. Vanoli, A novel hybrid polygeneration system supplying energy and desalinated water by renewable sources in Pantelleria Island, Energy (2017).

[6] A. Mohammadi, M. Mehrpooya, Energy and exergy analyses of a combined desalination and CCHP system driven by geothermal energy, Applied Thermal Engineering (2017).

[7] E. Akrami, A. Chitsaz, H. Nami, S. Mahmoudi, Energetic and exergoeconomic assessment of a multi-generation energy system based on indirect use of geothermal energy, Energy 124 (2017) 625–639.

[8] F. A. Boyaghchi, H. Safari, Parametric study and multi-criteria optimization of total exergetic and cost rates improvement potentials of a new geothermal based quadruple energy system, Energy Conversion and Management 137 (2017) 130–141.

[9] M. Akbari Kordlar, S. Mahmoudi, Exergeoconomic analysis and optimization of a novel co-generation system producing power and refrigeration, Energy Conversion and Management 134 (2017) 208–220.

[10] A. Mosaffa, N. H. Mokarram, L. G. Farshi, Thermo-economic analysis of combined different ORCs geothermal power plants and LNG cold energy, Geothermics 65 (2017) 113–125.

31

[11] O. A. Oyewunmi, C. J. Kirmse, A. M. Pantaleo, C. N. Markides, Performance of working-fluid mixtures in ORC-CHP systems for different heat-demand segments and heat-recovery temperature levels, Energy Conversion and Management 148 (2017) 1508–1524.

[12] D. Fiaschi, A. Lifshitz, G. Manfrida, D. Tempesti, An innovative ORC power plant layout for heat and power generation from medium- to low-temperature geothermal resources, Energy Conversion and Management 88 (2014) 883–893.

[13] M. Habka, S. Ajib, Determination and evaluation of the operation characteristics for two configurations of combined heat and power systems depending on the heating plant parameters in low-temperature geothermal applications, Energy Conversion and Management 76 (2013) 996–1008.

[14] F. Heberle, D. Brüggemann, Exergy based fluid selection for a geothermal Organic Rankine Cycle for combined heat and power generation, Applied Thermal Engineering 30 (2010) 1326–1332.

[15] T. Li, J. Zhu, W. Zhang, Comparative analysis of series and parallel geothermal systems combined power, heat and oil recovery in oilfield, Applied Thermal Engineering 50 (2013) 1132–1141.

[16] S. Van Erdeweghe, J. Van Bael, B. Laenen, W. D'haeseleer, Comparison of series/parallel configuration for a low-T geothermal CHP plant, coupled to thermal networks, Renewable Energy 111 (2017) 494–505.

[17] S. Van Erdeweghe, J. Van Bael, B. Laenen, W. D'haeseleer, Preheat-parallel configuration for low-temperature geothermally-fed CHP plants, Energy Conversion and Management 142 (2017) 117–126.

[18] M. Habka, S. Ajib, Investigation of novel, hybrid, geothermal-energized cogeneration plants based on organic Rankine cycle, Energy 70 (2014) 212–222.

[19] ITG, Informationsportal Tiefe Geothermie, 2017. URL: `www.tiefegeothermie.de/projekte`.

[20] IRENA, Renewable energy in district heating and cooling - Case studies, 2017. URL: `www.irena.org/remap`.

[21] S. Bos, B. Laenen, Development of the first deep geothermal doublet in the Campine Basin of Belgium, European Geologist 43 (2017) 16–20.

[22] D. Walraven, B. Laenen, W. D'haeseleer, Comparison of thermodynamic cycles for power production from low-temperature geothermal heat sources, Energy Conversion and Management 66 (2013) 220–233.

[23] G. van Rossum, Python Tutorial, Technical Report CS-R9526, Technical Report, Centrum voor Wiskunde en Informatica (CWI), Amsterdam, 1995. URL: `http://www.python.org`.

[24] J. Andersson, A General-Purpose Software Framework for Dynamic Optimization, Phd, Arenberg Doctoral School, KU Leuven, 2013. URL: `https://lirias.kuleuven.be/bitstream/123456789/418048/1/thesis_final2.pdf`.

[25] A. Wächter, L. T. Biegler, On the implementation of an interior-point filter line-search algorithm for large-scale nonlinear programming, Mathematical Programming 106 (2006) 25–57.

[26] E. Lemmon, M. Huber, M. McLinden, REFPROP - Reference Fluid Thermodynamic and Transport Properties. NIST Standard Reference Database 23, 2007.

[27] S. Van Erdeweghe, J. Van Bael, B. Laenen, W. D'haeseleer, Optimal Configuration for Low-T Geothermal CHP Plants, in: GRC Transactions, Vol. 41, Salt Lake City, 2017, pp. 2110–2125. URL: `https://www.mech.kuleuven.be/en/tme/research/energy_environment/PublicationsEnergyandenvironment/Journalpapers`.

[28] Y. Dai, J. Wang, L. Gao, Parametric optimization and comparative study of organic Rankine cycle (ORC) for low grade waste heat recovery, Energy Conversion and Management 50 (2009) 576–582.

[29] J. Calm, G. Hourahan, Physical, Safety and Environmental Data for Current and Alternative Refrigerants, in: International Congress of Refrigeration, Prague, Czech Republic, 2011. URL: `http://www.hourahan.com/wp/wp-content/uploads/2010/08/2011-Physical-Safety-and-Environmental-Data2.pdf`.

[30] M. Imran, M. Usman, B.-S. Park, Y. Yang, Comparative assessment of Organic Rankine Cycle integration for low temperature geothermal heat source applications, Energy 102 (2016) 473–490.

[31] R. Gabbrielli, A novel design approach for small scale low enthalpy binary geothermal power plants, Energy Conversion and Management 64 (2012) 263–272.

[32] G. Blöcher, S. Kranz, G. Zimmermann, S. Frick, A. Hassanzadegan, I. Moeck, W. Brandt, A. Saadat, E. Huenges, Conceptual Model for Coupling Geothermal Power Plants with Deep Reservoirs, in: World Geothermal Congress, April, Bali, Indonesia, 2010, pp. 25–29.

[33] A. Franco, Power production from a moderate temperature geothermal resource with regenerative Organic Rankine Cycles, Energy for Sustainable Development 15 (2011) 411–419.